Neoplasia 59 (2025) 101074

Contents lists available at ScienceDirect

Neoplasia

journal homepage: www.elsevier.com/locate/neo

Original Research

Early separation and parallel clonal selection of dedifferentiated and well-differentiated components in dedifferentiated liposarcoma

Tetsuya Sekita [a,b,c], Naofumi Asano [a,c,*], Takashi Kubo [a,d], Hirohiko Totsuka [e], Sachiyo Mitani [a], Naoko Hattori [f,g], Akihiko Yoshida [h], Eisuke Kobayashi [b], Motokiyo Komiyama [i], Toshikazu Ushijima [f,g], Robert Nakayama [c], Masaya Nakamura [c], Akira Kawai [b], Hitoshi Ichikawa [a,*]

[a] Department of Clinical Genomics, National Cancer Center Research Institute, Tokyo, Japan
[b] Department of Musculoskeletal Oncology, National Cancer Center Hospital, Tokyo, Japan
[c] Department of Orthopaedic Surgery, Keio University School of Medicine, Tokyo, Japan
[d] Department of Laboratory Medicine, National Cancer Center Hospital, Tokyo, Japan
[e] StaGen Co., Ltd, Tokyo, Japan
[f] Division of Epigenome, National Cancer Center Research Institute, Tokyo, Japan
[g] Department of Epigenomics, Institute for Advanced Life Sciences, Hoshi University, Tokyo, Japan
[h] Department of Diagnostic Pathology, National Cancer Center Hospital, Tokyo, Japan
[i] Department of Urology, National Cancer Center Hospital, Tokyo, Japan

ARTICLE INFO

Keywords:
DDLPS
Dedifferentiation
Clonal evolution
Multiregion analysis
Phylogenetic tree

ABSTRACT

Dedifferentiated liposarcoma (DDLPS) comprises a high-grade dedifferentiated (DD) component and a juxtaposed well-differentiated (WD) component. The DD component is believed to originate from the WD component by acquiring additional genomic alterations. In this study, we performed multiregion genome, epigenome, and transcriptome analyses of three patients with DDLPS. In two patients, there were few common genomic alterations across all samples, but many common alterations within DD or WD component samples. Phylogenetic trees predicted from the genomic alterations were consistent with those predicted from DNA methylation patterns. The expression patterns of adipogenesis-related genes differed between DD and WD components and also among patients in connection with their CpG island methylation status. These results indicate that in some patients, WD and DD components are evolutionarily separated at very early stages of tumorigenesis, and are formed through relatively long clonal selection with acquisition of different driver genomic alterations and DNA methylation changes.

Introduction

Liposarcoma accounts for ~20 % of all malignant mesenchymal neoplasms [1]. Liposarcoma shows histologic and genetic variability and has been classified into five subtypes: well-differentiated liposarcoma (WDLPS), dedifferentiated liposarcoma (DDLPS), myxoid liposarcoma, pleomorphic liposarcoma, and myxoid pleomorphic liposarcoma [2]. DDLPS accounts for ~10 % of liposarcomas, with an incidence of <0.1/million cases each year [3]. DDLPS manifests as two morphologically distinct components: an often high-grade non-lipogenic (dedifferentiated, DD) component and a juxtaposed well-differentiated (WD) component [4,5]. Surgical excision remains the standard of care for localized DDLPS, because the tumors are largely resistant to conventional cytotoxic chemotherapy [6]. Local recurrence is observed in ≥40 % of all cases and almost all cases with retroperitoneal locations [2]. While DD components have relatively well-defined margin, WD components often have indistinct margin with the surrounding adipose tissue, contributing to the high rate of local recurrence. During follow-up, distant metastases are observed in 15 %–20 % of the cases, associated with considerably worse prognosis, with an overall mortality rate of 28 %–56 % at the five-year follow-up [7].

Because DDLPS occurs in ~10 % of cases initially diagnosed as WDLPS [8] and amplification of the 12q13-15 chromosomal region, including *MDM2* and *CDK4*, is a common feature of WDLPS and both

* Corresponding authors.
E-mail addresses: nasano@keio.jp (N. Asano), hichikaw@ncc.go.jp (H. Ichikawa).

https://doi.org/10.1016/j.neo.2024.101074
Received 29 August 2024; Received in revised form 12 October 2024; Accepted 15 October 2024
1476-5586/© 2024 The Authors. Published by Elsevier Inc. This is an open access article under the CC BY-NC-ND license (http://creativecommons.org/licenses/by-nc-nd/4.0/).

components of DDLPS [9–11], it is generally assumed that the DD component in DDLPS develops from a subclone in the preexisting WD component. The *MDM2* and *CDK4* genes are located on separate amplicons [12,13], and high-level amplification of *CDK4* has been reported to be a factor for poor prognosis in DDLPS [14]. The Cancer Genome Atlas (TCGA) Research Network analyzed 50 DDLPS cases in a comprehensive molecular profiling study of 206 soft tissue sarcomas. The study revealed that DDLPS can be divided into prognostic subgroups based on their copy number aberrations (CNAs) and DNA methylation status [15]. Frequent CNAs were found in genes that inhibit adipocyte differentiation, such as *JUN* (42 %), *DDIT3* (32 %), *PTPRQ* (46 %), *YAP1* (16 %), and *CEBPA* (24 %), and genes located at 12q13-15 [15]. Subsequently, we performed genomic and transcriptomic analysis of 115 DDLPS samples (including 50 DDLPS samples from TCGA) and paired WD component samples from eight patients and reported CNA-based prognostic subgrouping, as well as novel *DNM3OS* fusions in some DDLPS cases [16]. Comparative analysis of WD and DD component samples revealed that few point mutations, but more CNAs, were shared between the two components. The expression of cell cycle progression-related genes was enhanced in the DD component but have not reported obvious genomic alterations that could trigger dedifferentiation in DD samples.

Multiregion cancer genomic analyses have been used to assess intratumor heterogeneity by multiple sampling within the same patient in many tumor types [17]. Such analyses allow us to create a tumor phylogenetic tree based on somatic mutations to estimate clonal evolution in the tumor [18–22]. Estimating clonal evolution can lead to the identification of genomic alterations that are essential for cancer evolution [21]. While rarity of common point mutations between WD and DD components was reported as described above, no studies have analyzed the clonal evolution of DDLPS using multiregion samples.

Here, we evaluated the intra-tumor heterogeneity of DDLPS by multiregion analysis in three patients to evaluate clonal evolution. This approach revealed an unexpected, early separation and parallel clonal selection of WD and DD clones in DDLPS development and provided insights useful for therapeutic strategy.

Material and methods

Patients and tumor samples

Three patients diagnosed with DDLPS and whose tumor tissue samples were suitable for multiregion analysis were enrolled in the study (Supplementary Table S1). The eligibility criteria were as follows: (1) Pathologically confirmed diagnosis of dedifferentiated liposarcoma, (2) large tumor size, and (3) clear boundary between components. These patients underwent R0 or R1 resection at the National Cancer Center Hospital (NCCH, Tokyo, Japan). We cut out tumor samples from 10 separate locations of the resected tumor from each patient and snap-froze them. Adjacent normal tissue samples (patients 1 and 2) and a blood sample (patient 3) were used as controls. The Institutional Review Board of the National Cancer Center approved the study (protocol number 2004-050). All patients provided written informed consent. The follow-up periods were 2–46 months. Clinical outcomes were dead of disease for patient 1, lost of follow-up (disease-free at 2 months after surgery) for patient 2, and alive with disease for patient 3. Recurrence was observed in patient 1, and metastasis was seen in patient 3 (Supplementary Table S1). Only patient 1 received neoadjuvant chemotherapy (1 course of adriamycin and ifosfamide and 1 course of adriamycin) from 51 days to 24 days before surgical resection. Her tumor progressed after the chemotherapy without large tumor necrosis (necrosis rate: ~20 %). Snap-frozen tumor samples and control normal tissue samples were ground using a Multi-bead Shocker (Yasui Machine, Osaka, Japan) and to prepare genomic DNA and total RNA. Genomic DNA was prepared using the standard phenol–chloroform extraction and ethanol precipitation methods. Total RNA was extracted using ISOGEN reagent (Nippon Gene, Tokyo, Japan) and purified using RNeasy MinElute Cleanup Kit (Qiagen, Hilden, Germany) according to the manufacturer's protocol. Control genomic DNA from the blood sample was prepared using a FlexiGene DNA Kit (Qiagen).

Pathology review

All samples underwent detailed pathology review, including delineation of WDLPS and DDLPS features within a sample, to confirm diagnosis by an expert sarcoma surgical pathologist.

Whole-exome sequencing (WES) analysis

Sequencing libraries were prepared using SureSelect Human All Exon V5, SureSelect XT Reagents (Agilent Technologies, St. Clara, CA, USA), and KAPA Hyper Prep Kit (KAPA Biosystems, Wilmington, MA, USA) from 0.2 μg of DNA, according to the manufacturer's protocol. Paired-end sequencing (2 × 150 bases) was performed on a NovaSeq 6000 sequencer (Illumina, San Diego, CA, USA). The sequence reads were aligned to the human reference genome (GRCh38/hg38) using the Burroughs–Wheeler Aligner-MEM algorithm [23]. The average read depths were 144.1–274.1. Mutations (SNVs and indels) were detected using MuTect2 version 4.1.6 [24]. Mutation candidates that did not fit the pattern were manually inspected using Integrative Genomics Viewer [25]. CNAs were analyzed using the Allele-Specific Copy number Analysis of Tumours program (ASCAT) [26]. The estimated copy numbers were normalized by dividing the median ploidy and doubling. The log R ratio was calculated using data from the control pool, with tangent normalization to reduce noise. When ASCAT's estimates of ploidy and purity were clearly inappropriate, they were manually curated. To count these CNAs as mutations, we made bar graphs of CNAs across the entire genome and then manually resolved the obtained CNA patterns to genomic alteration events (Supplementary Fig. S4).

DNA methylation analysis

Genome-wide DNA methylation analysis was performed using the Infinium MethylationEPIC BeadsChip (Illumina) platform, as described [27]. Data were processed using GenomeStudio Methylation Module Software (Illumina) (V.1.9.0 2011.1) and the MACON web tool [28] for intra-array normalization with a peak-based correction method (BMIQ). To reduce data size and obtain data that were easier to handle, the CpG probes were grouped into genomic blocks, which consisted of probes within 500 bp, using MACON.

Phylogenetic trees

The phylogenetic trees were drawn using the fastme.bal function in the R package "ape." Genomic alteration-based phylogenetic trees were constructed using the numbers of mutations and CNA events as Euclidean distance. Methylation-based phylogenetic trees were inferred using the minimal evolution method [29]. The top 1 % of CpG sites with the greatest intratumoral methylation range were used.

RNA sequencing analysis

For RNA sequencing, we adopted an exome capture sequencing method. Sequencing libraries were prepared from 0.2 μg of total RNA using SureSelect Human All Exon V5 and SureSelect XT HS2 RNA Reagent Kit (Agilent Technologies). Paired-end sequencing (2 × 150 bases) was performed on NovaSeq 6000 sequencers (Illumina). For gene expression analysis, sequencing reads were aligned to the human reference genome (GRCh38/hg38) using STAR v.2.7.3a [30], and the TPM value for each gene was calculated using StringTie. GSEA was performed using the JAVA GSEA v.3.0 program [31]. Gene fusions were searched using STAR-Fusion v.1.9.1 [30]. GSEA was performed using

gene sets from the Molecular Signatures Database (https://www.gsea-msigdb.org/gsea/msigdb/index.jsp). We picked a set of genes from curated gene sets (C2) and hallmark (H) genes related to adipogenic differentiation.

Statistical analysis

Statistical analyses were performed using GraphPad Prism 8 (GraphPad, San Diego, CA, USA). Two-group comparisons were performed using unpaired or one-sided paired *t*-test. P-values less than 0.05 were considered statistically significant.

Data availability

The data generated in this study are publicly available in NBDC Human Database at JGAS000759 and within the supplementary files.

Results

Clinical characteristics and sampling details of the study participants

Patients 1–3 (two males and one female) were included in the study. Their ages at operation were 54–73 years. The maximum tumor diameters were 22.9–30.7 cm. Only patient 1 underwent neoadjuvant chemotherapy (see Materials and Methods) before surgical resection. Patients 2 and 3 were treated with surgical resection without prior therapy (Supplementary Table S1).

We collected samples from 10 locations (T01–T10) of the resected tumor (Fig. 1a). Pathological evaluation of the DD component showed that patients 1 and 2 had myogenic differentiation and patient 3 had osteogenic differentiation. The breakdown of WD and DD in each patient was as follows: 3 WD (T01–03) and 7 DD (T04–10) in patients 1 (Fig. 1b) and 2 (Supplementary Fig. S1a); 5 WD (T06–10) and 5 DD (T01–05) in

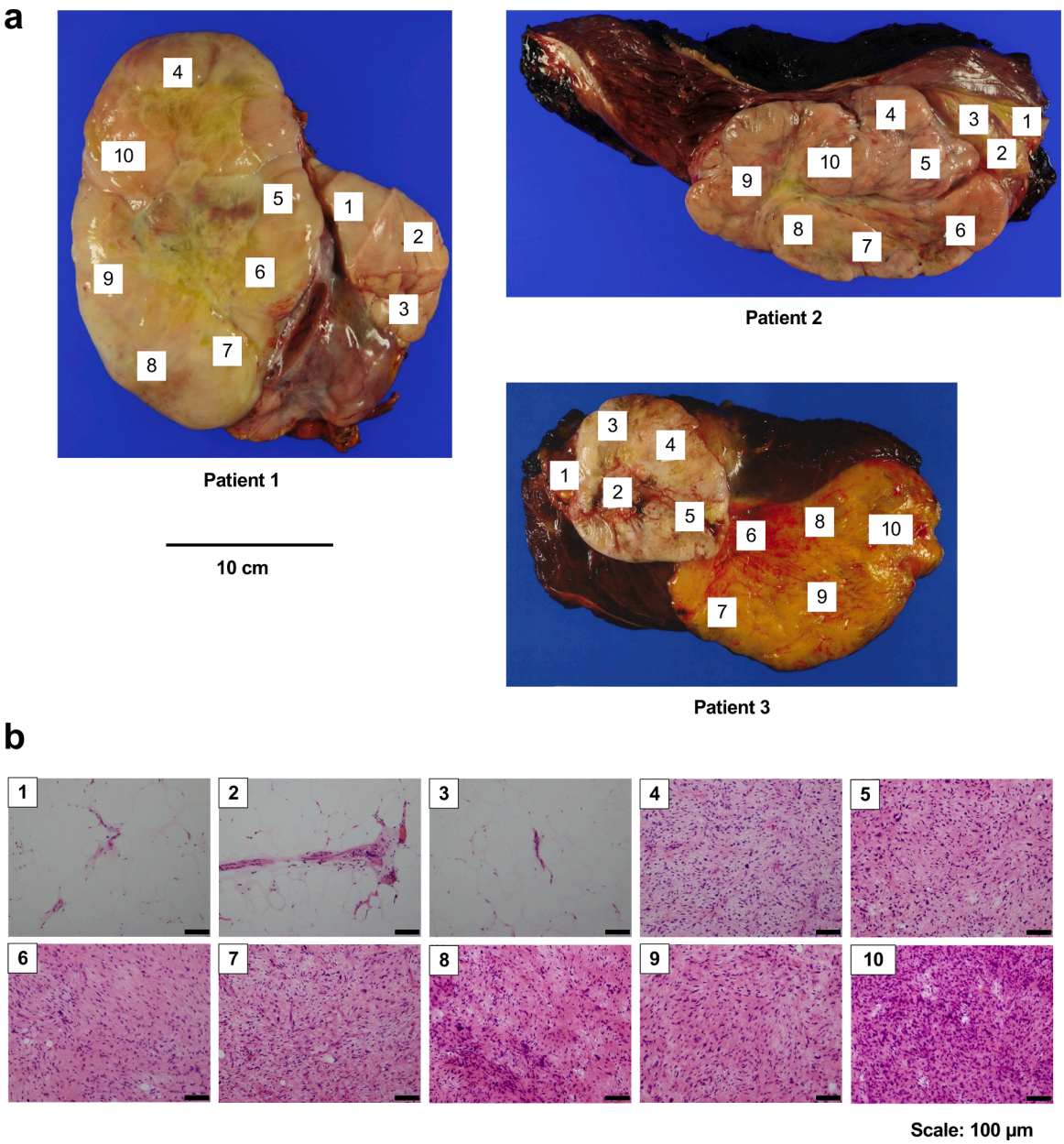

Fig. 1. Sample locations and pathological findings.
a. Tumor samples were obtained from 10 anatomically distinct regions of each tumor to assess spatial genomic heterogeneity. **b.** Pathological images of WD (1–3) and DD (4–10) samples from patient 1.

patient 3 (Supplementary Fig. S1b). We extracted DNA and RNA from these samples and performed whole-exome sequencing (WES), RNA sequencing (RNA-Seq), and DNA methylation microarray analyses. Sample T02 from patient 3 was excluded because sufficient DNA could not be extracted, probably due to marked osteogenic differentiation (Supplementary Fig. S1b).

Somatic mutations

Somatic mutations (single nucleotide variants [SNVs] and short insertions/deletions) were detected from the WES data (see Materials and Methods). The average number of somatic mutations identified in the WD and DD components were 39 and 50 in patient 1, 17 and 46 in patient 2, and 19 and 90 in patient 3, respectively (Supplementary Table S2). Significantly more mutations were detected in the DD component in all patients ($P = 0.0015$, 0.0004, < 0.0001) (Fig. 2a).

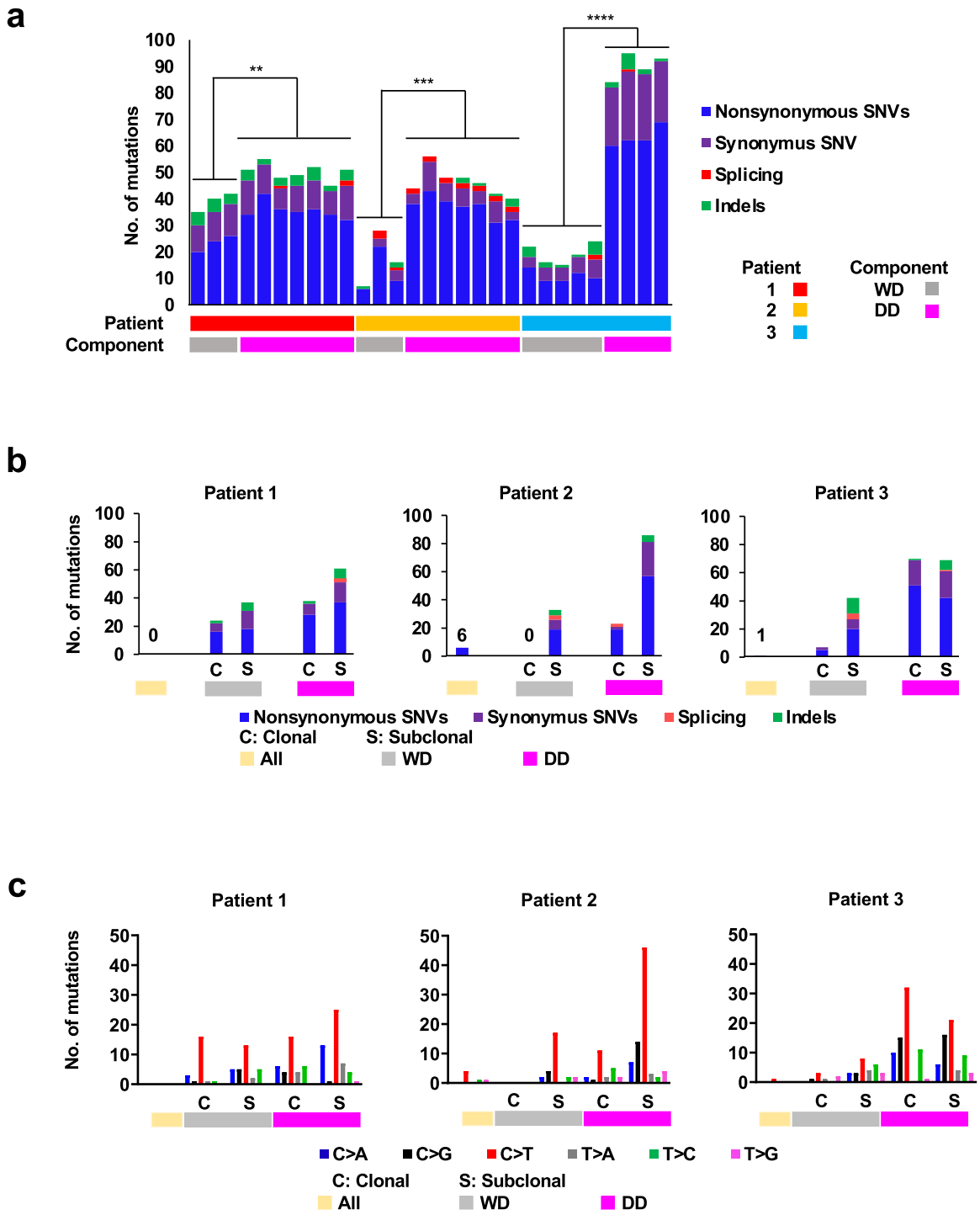

Fig. 2. Characteristics of somatic mutations.
a. Somatic mutations (SNVs and indels) of each sample were classified into nonsynonymous SNVs, synonymous SNVs, splice site SNVs, and indels. $^{**}P < 0.01$, $^{***}P < 0.001$, and $^{****}P < 0.0001$ by an unpaired *t*-test. **b.** Somatic mutations were classified into common, clonal, and subclonal mutations for each patient. **c.** SNVs were classified according to six base substitution patterns: C > A, C > G, C > T, T > A, T > C, and T > G.

Some of these differences are attributable to the low tumor cell content of the WD samples, which was expected from their low variant allele frequencies (Supplementary Fig. S2). However, the detected mutations were shared to various degrees among the samples within each patient. These mutations could be categorized into those shared by all samples (common mutations), those shared by all WD or DD samples (WD-clonal or DD-clonal mutations, respectively), and those found in some WD or DD samples (WD-subclonal or DD-subclonal mutations, respectively). Common mutations were very few (0 in patient 1, 6 in patient 2, and 1 in patient 3) (Fig. 2b). WD-clonal mutations were relatively few (24 in patient 1, 0 in patient 2, and 7 in patient 3) (Fig. 2b), and more DD-clonal mutations were detected (38 in patient 1, 23 in patient 2, 70 in patient 3) (Fig. 2b). Although some of these DD-clonal mutations were expected to be involved in dedifferentiation (DD component formation), we were unable to find any correlation between mutated genes and adipogenic pathways. Excluding the common mutations, there were no shared mutations between WD and DD samples.

C > T transitions were the most frequent mutations in all categories. This trend was consistent between the WD and DD samples (Fig. 2c).

Somatic copy number alterations

Genome copy numbers of each tumor sample were estimated from the WES data (see Materials and Methods). CNA patterns, mainly comprising focal amplifications, were similar between multiple samples within each patient, and differed widely between patients (Fig. 3a). Many CNAs were shared by all samples (common CNAs), all WD samples (WD-clonal CNAs), and all DD samples (DD-clonal CNAs) in each patient. When the loci of common CNAs were compared between patients, only 12q13-15 was commonly amplified among the three patients (Fig. 3a and Supplementary Fig. S3). The amplification of 12q13-15 is a hallmark CNA of DDLPS and WDLPS; *MDM2* and *CDK4* are representatives of amplified genes at this locus. Their copy numbers were generally higher in DD samples than in WD samples (Fig. 3b). The copy number differences between WD and DD samples were larger in *CDK4* than *MDM2* (Fig. 3b). Two loci were commonly amplified in two patients: 1q21 (patients 2 and 3) and 12q21 (patients 1 and 2). Amplified genes at these loci are expected to be involved in early tumorigenesis, but there were no oncogenes in these regions. Then, we compared DD-clonal CNA loci between patients. Although no loci were common to all three patients, 19p13 was commonly amplified in patients 1 and 2. Amplified genes at this locus are expected to be involved in dedifferentiation, but we could not detect genes functionally relevant to anti-adipogenic pathways.

The CNAs were resolved to genomic alteration events and counted (an example is shown in Supplementary Fig. S4). Six to 45 CNA events were identified in 29 tumor samples. The events were classified similar like somatic mutations and CNA patterns. We detected 4, 21, and 1 common CNA events; 13, 0, and 5 WD-clonal events; and 17, 3, and 12 DD-clonal events in patients 1, 2, and 3, respectively (Supplementary Fig. S5) (Supplementary Table S3).

Phylogenetic tree

To determine clonal evolution in the three DDLPS tumors, we constructed phylogenetic trees based on the somatic mutations and CNA events identified (Fig. 3c). In patients 1 and 3, the trunks were very short, suggesting that the WD and DD samples were separated at a very early stage of tumorigenesis. After separating the WD and DD component samples was complete, both components had sub-trunks longer than the original trunks, suggesting the existence of long-term clonal selection in formation of WD and DD component tumors. DD sub-trunks were longer than WD sub-trunks in both patients. In patient 2, the main trunk was relatively long, and a WD sub-trunk had not formed, suggesting that the DD clones originated from a WD sub-clone. A comparison of the phylogenetic tree and macroscopic locations of the samples showed that samples with similar genetic abnormalities were present at neighboring locations within each component. For example, in patient 1, samples T07 and T08; T04 and T10; and T05 and T06 were adjacent, forming three subgroups (Figs. 1a and 3c).

DNA methylation aberrations

We used methylation microarrays to perform DNA methylation analysis on 29 tumor samples and six control normal adipose tissue samples from non-relevant patients. The methylation data (β-values) obtained with 865,859 probes were summarized into 551,478 genomic blocks. A t-SNE analysis using the β-values of all blocks showed that the WD and DD samples of each patient and normal samples formed clusters (Fig. 4a). Although the three WD clusters were close to each other and a normal cluster, the three DD clusters were relatively separated. An unsupervised hierarchical clustering analysis using the β-values of the top 50,000 blocks with high variability revealed that the WD samples clustered together with the normal samples, and the DD samples of the three patients formed distinct clusters (Fig. 4b). These three DD clusters were characterized by low methylation in large groups of methylation blocks, which differed among the three patients, suggesting that DNA demethylation of large regions occurred in a patient-specific manner.

We constructed a phylogenetic tree for each patient using the β-values of the top 5,000 CpG island blocks with high variability (Fig. 4c). Compared with the genomic alteration-based phylogenetic tree (Fig. 3c), these trees showed statistically significant similarity ($P =$ 0.00003, 0.00004, and 0.0002 in patients 1, 2, and 3, respectively).

Association of gene expression with DNA methylation

Gene expression was compared using transcripts per million (TPM) values calculated from RNA-Seq data. Gene expression analysis excluded T07 from patient 2 and T01 from patient 3 due to poor RNA quality. Principal component analysis (PCA) using the major PCs (PC1 and PC2) (Supplementary Fig. S6a) and unsupervised hierarchical clustering analysis using all gene data (not shown) did not show clear clustering of WD and DD samples, unlike DNA methylation analysis. Conversely, gene set enrichment analysis (GSEA) revealed significant differences in the expression of "adipogenesis" genes (Supplementary Table S4 and Supplementary Fig. S7). PCA with PC3 and PC4 (Supplementary Fig. S6b) and hierarchical clustering with adipogenesis-related genes (Fig. 5a) showed patient-specific clustering of samples within the WD and DD clusters, suggesting patient-specific expression patterns. Therefore, we evaluated the differences between the WD and DD components of each patient in terms of expression of adipogenesis-related genes with a volcano plot (Fig. 5b). Highly expressed genes in DD samples differed among the three patients (Fig. 5c). *VEGFD, BMP7*, and *NR2F1* in patient 1 and *COL11A1, COL7A1*, and *KCNH2* in patient 3 were highly expressed. When the expression of these genes was examined in 34 DDLPS tumors from our study [16], high expression was observed in some patients (Supplementary Fig. S8). We examined a possibility that these patient-specific high expression patterns may be related to the patient-specific DNA demethylation patterns in Fig. 4b. In the methylation status of the highly expressed genes, four and six genes were specifically demethylated in patients 1 and 3, respectively (Fig. 5c). *BMP7, NR2F1*, and *COL11A1* were included (Fig. 5d).

Mechanisms of dedifferentiation

We examined the CNA states of genes that inhibit adipocyte differentiation. *DDIT3* was commonly amplified in the DD samples of patient 1, and *JUN* was amplified in the DD samples of patient 2 (Supplementary Fig. S9). *DDIT3* expression was enhanced in the amplified samples (Supplementary Fig. S9). These findings suggest that the amplification of *DDIT3* and *JUN* was involved in dedifferentiation during DDLPS development in patients 1 and 2, respectively.

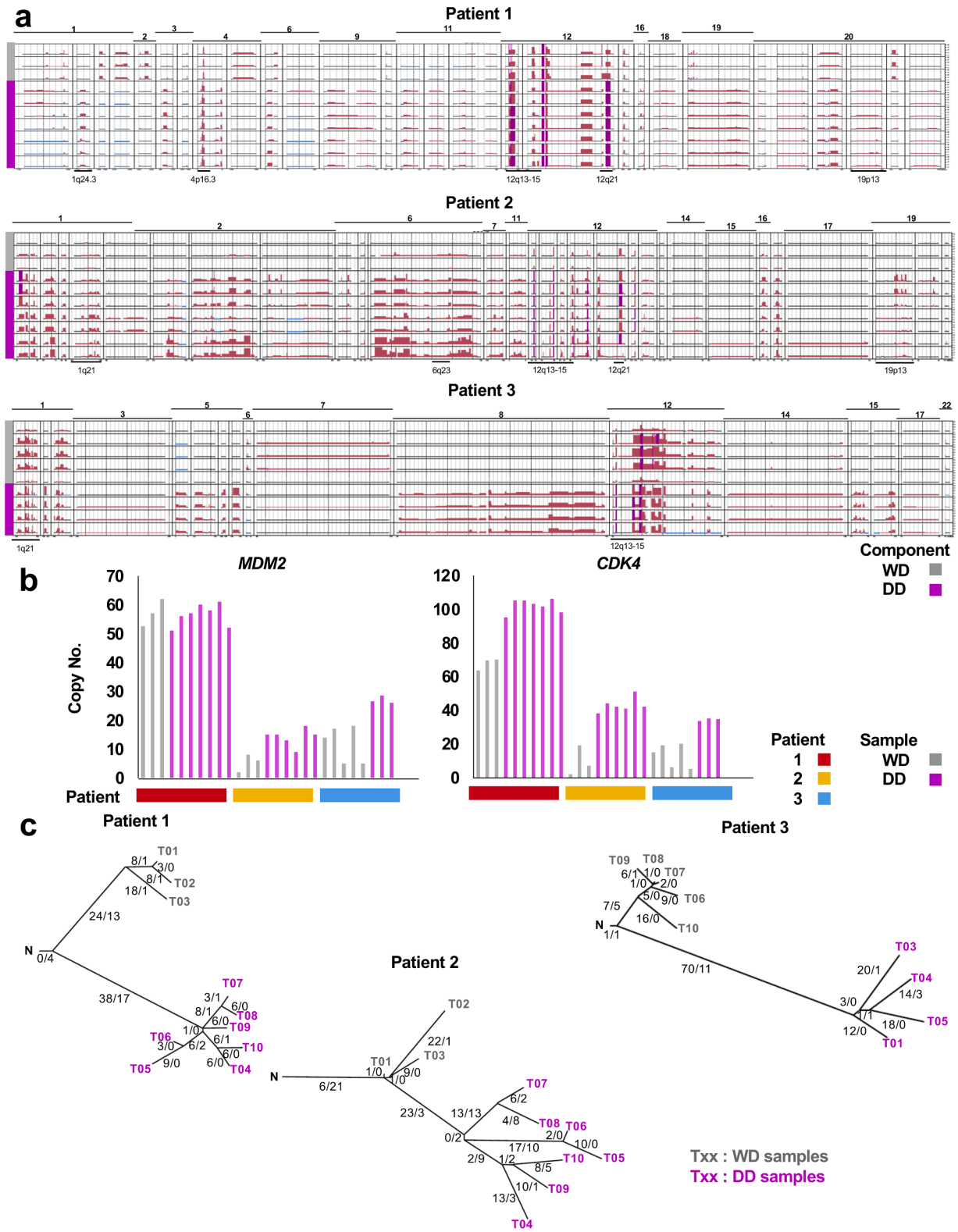

Fig. 3. CNA patterns and genomic alteration-based phylogenetic trees.
a. CNA patterns across the genome. Chromosomal regions where major CNAs were observed are shown. Red indicates segment gain (≥3), purple indicates altitude amplification (≥20), and blue indicates segment loss (=1). Horizontal and vertical axes indicate chromosome position and copy number, respectively. **b.** Copy numbers of *MDM2* and *CDK4* in each sample. **c.** Phylogenetic trees constructed using genomic alterations. Numeric values on each stem indicate the number of somatic mutations (left) and CNA events (right).

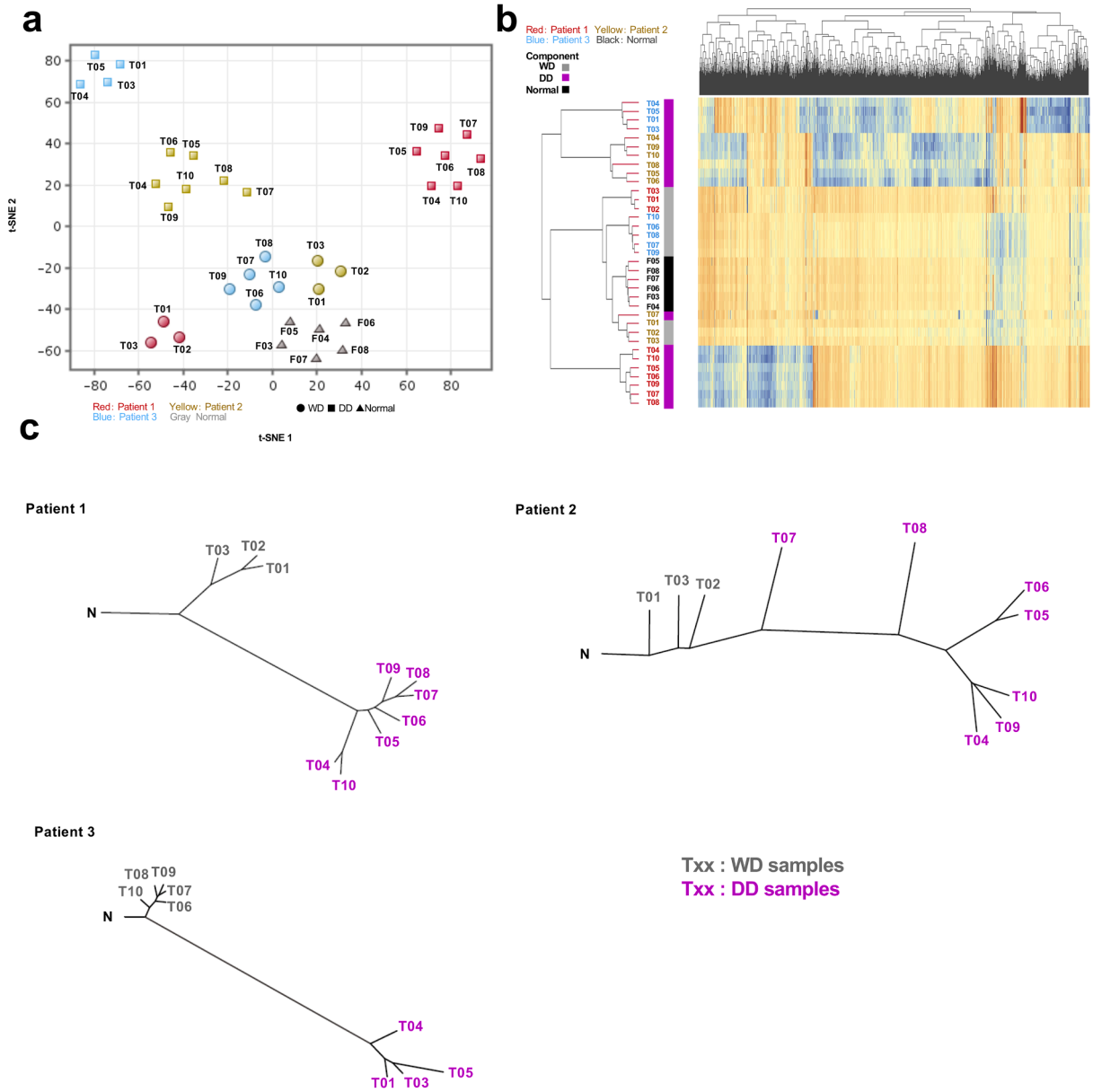

Fig. 4. DNA methylation patterns and phylogenetic trees.
a. t-SNE analysis of all DDLPS and 6 normal adipose tissue samples. **b.** Unsupervised hierarchical clustering based on the top 50,000 genomic blocks with a high variety of β-values. **c.** Phylogenetic trees constructed using the top 5,000 CpG island probes with a high variety of β-values.

A comparison of whole WD and whole DD samples by GSEA revealed enrichment of cell cycle-related gene sets, including G2M checkpoint and E2F targets, in the DD samples (Supplementary Table S4). *CDK4*, an upstream activator of Rb/E2F signaling, was more markedly amplified in DD than WD samples (Fig. 3b). Moreover, *CDK4* expression was enhanced in DD samples (Supplementary Fig. S10). Therefore, enhanced amplification and expression of *CDK4* may contribute to dedifferentiation.

DNM3OS fusion was expected to be involved in dedifferentiation [16], but was only detected in a few DD samples (Supplementary Fig. S11). *DNM3OS* fusion is likely involved in tumor progression but not dedifferentiation.

Discussion

It has been assumed that DDLPS is caused by the appearance and expansion of a DD clone in a preexisting WD tumor, resulting in the formation of a DD component. In this study, multiregion genome analysis showed that WD and DD clones branched off at a very early stage in tumorigenesis, after which they underwent separate and relatively long clonal evolution in two of the three DDLPS tumors examined. Additionally, the expression patterns of adipogenesis-related genes were similar among the DD samples of each patient, but varied between patients, and associated with the DNA methylation patterns.

Multiregion analyses have been performed on a variety of cancers. These studies have revealed the clonal evolution of these tumor types and provided novel insights, including the association between heterogeneity and prognosis, as well as the presence of heterogeneity in important oncogene abnormalities [20,22]. Although multiregion analyses from the same tumor have not been reported in DDLPS, some reports, including our previous study [16], have compared single WD and DD samples from the same patient. In these studies, there were few common mutations between the WD and DD components. Beird *et al.* [10] analyzed 17 patients with DDLPS and reported that only 8.3 % of

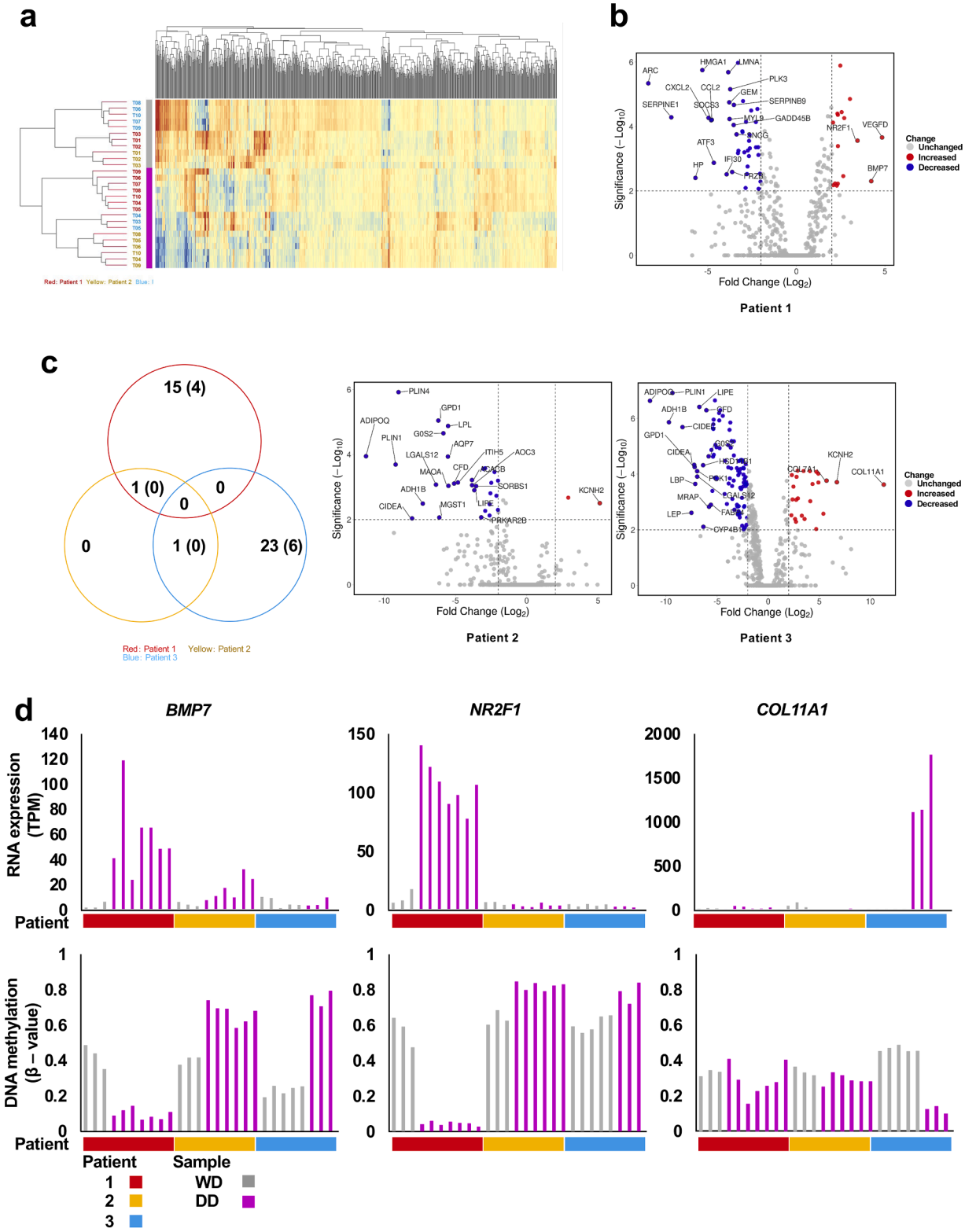

Fig. 5. Gene expression and its association with DNA methylation.

a. Unsupervised hierarchical clustering based on the expression of adipogenic differentiation-related genes. **b.** Volcano plots of adipogenic differentiation-related genes. Red and blue dots denote high fold-change (>4 or <1/4; horizontal axis) and high statistical significance ($P < 0.01$ by one-sided paired *t*-test; vertical axis), respectively. **c.** Venn diagram showing the number of adipogenic differentiation-related genes highly expressed in the DD components. The number of DD clonal demethylated genes is within parentheses. **d.** RNA expression (top row) and DNA methylation (bottom row) of three genes with marked expression differences between the WD and DD components in patients 1–3.

the WD component mutations were shared with the DD component. Additionally, the DD component had higher numbers of copy number loss and amplifications. In our previous study of eight patients [16], we observed very few common mutations, a relatively higher number of common CNAs, and more prominent CNAs and chromosomal rearrangements in the DD component. The results of our multiregion analysis were consistent with these reports and additionally revealed that many mutations and CNAs were shared within all samples of each component, except the WD component of patient 2. This finding indicates that WD and DD components evolved in parallel after early separation into two components in patients 1 and 3.

We present a schematic representation of the clonal evolution of DDLPS (Fig. 6). Fig. 6a shows the classic model. First, an ancestral WD clone is generated, which expands and diversifies into multiple clones, and then a DD clone is generated from a WD subclone. The tumor from patient 2 follows this model. Fig. 6b shows the new model proposed in this study. First, a common progenitor clone is generated, which separates into ancestral WD and ancestral DD clones at a very early stage of tumorigenesis. Then, both clones evolve through relatively long and independent clonal selection, and finally form WD and DD component tumors with heterogeneity to become DDLPS. The tumors from patients 1 and 3 match this model. The former classic model account for occurrence of DDLPS in initially diagnosed as WDLPS [8] and some part of *de novo* DDLPS such as patient 2. On the other hand, the latter early segregation type, which we proposed in this study, can explain the occurrence of the remaining *de novo* DDLPS such as patients 1 and 3. Very recently a study that performed single-cell RNA-Seq analysis of DDLPS and evaluated its tumor cell heterogeneity was reported by Gruel et al. [32] . This study showed that DD and WD components derive early from this ancestral progenitor and later acquire additional private clonal and subclonal CNVs, which is consistent with our findings.

Various models of tumor evolution, including linear, branching, neutral, and punctuated evolution, have been proposed [33]. The classic model in Fig. 6a follows linear evolution, characterized by step-wise acquisition of mutations leading to increased malignancy. The new model in Fig. 6b is a kind of branching evolution that involves divergent clonal lineages evolving in parallel from a common ancestor, with multiple clones expanding simultaneously due to increased fitness. Although branching evolution has been reported in various human malignant tumors, such as breast cancer, melanoma, and kidney cancer [22,34,35], that in DDLPS is unique in terms of separation at a very early stage and relatively long clonal selection. The co-existence of subclones in branching evolution raises a possibility of cooperation between subclones [33]. Actually, such clonal cooperation has been reported in several tumors. Vinci *et al.* [36] generated subclonal patient-derived models for pediatric glioblastoma and diffuse intrinsic pontine glioma in vitro and in vivo. They observed that these different subclones interacted to promote tumorigenesis. However, it is still unknown how WD and DD components cooperate to each other in DDLPS.

To analyze the mechanisms of dedifferentiation, we extracted the DD-clonal genomic alterations found in all DD samples but not in all WD samples. First, no known genes involved in adipogenesis regulation were included in the DD-clonal mutations identified in each patient (Fig. 2b). Second, DD sample-specific *DDIT3* and *JUN* amplification were observed. The genomic amplification of *JUN* has been implicated in progression from WDLPS to DDLPS [37], which blocks adipocyte differentiation at an early step [38]. *DDIT3* is a member of the CCAAT/enhancer-binding protein family of genes, postulated to act as a dominant-negative regulator of other CCAAT/enhancer-binding proteins [39]. Additionally, its amplification appears to interfere with the adipogenic molecular program [40]. Additionally, in all patients examined, *CDK4* was more highly amplified and expressed in the DD component (Fig. 3b and Supplementary Fig. S9). The resulting enhanced cell cycle progression may also contribute to dedifferentiation.

The extent of epigenetic changes occurring alongside the clonal evolution of DDLPS is largely unknown. In analyses of advanced prostate cancer [41] and lung cancer [19], the phylogenetic trees generated with CNAs were similar to those generated with DNA methylation alterations, and the phylogenetic trees based on genomic alterations and DNA methylation were similar between patients. The expression of genes involved in adipogenic differentiation that characterize each patient was correlated to their promoter DNA methylation. Conversely, although the DNA methylation patterns of WD component samples were similar, those of DD component samples were relatively different among patients. These results suggest that different molecular triggers that cause dedifferentiation may generate and maintain different epigenomic states.

High *BMP7* and *NR2F1* expression is characteristic of the DD component in patient 1. BMP7, also called osteogenic protein-1, is a member of the TGF-β family of proteins and is involved in bone

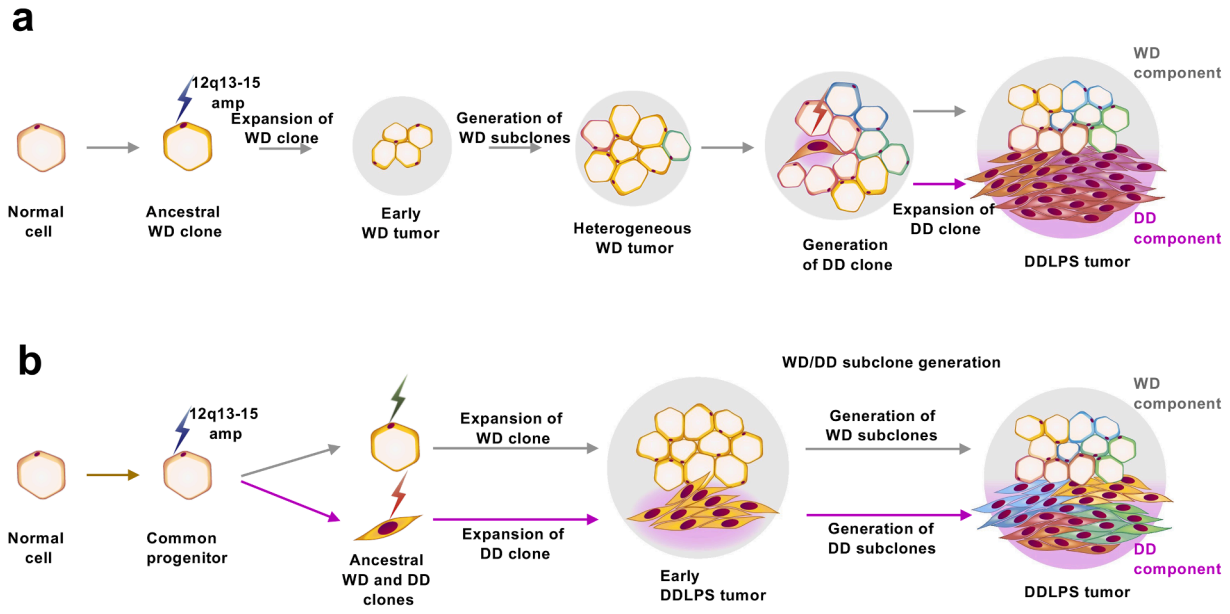

Fig. 6. Scheme showing the clonal evolution of DDLPS.
The classic model (**a**) and the new model proposed in this study (**b**) for clonal evolution of DDLPS. The WD tumor is in gray; the DD tumor is in pink.

formation. BMP7 is involved in forming brown fat [42], and the TGF-β/BMP superfamily regulates adipogenesis from mesenchymal stem cells through the glucocorticoid receptor [43]. *BMP7* is highly expressed in various sarcomas, such as osteosarcoma, synovial sarcoma, and alveolar soft part sarcoma [44]. *NR2F1* was reported to inhibit adipogenesis [45], through unknown mechanisms. In patient 3, *COL11A1* was highly expressed in all DD samples. Shaik *et al.* reported that *COL11A1* is highly expressed in adipose-derived stem cells when differentiation is induced toward osteogenesis compared with adipogenesis [46]. This is consistent with the osteogenic differentiation of the DD component in patient 3. Transition into the adipose-derived stem cell stage may have occurred in association with dedifferentiation in patient 3.

In this study, we found that both of WD and DD components are formed through relatively long clonal selection in some part of DDLPS. During such parallel clonal evolution, the WD and DD clones that acquire distinct driver genomic alterations are expected to be selected and to form WD and DD components, respectively. Because *MDM2* amplification and *CDK4* amplification are trunk genomic alterations that exist in both components, MDM2 inhibitors and CDK4 inhibitors whose clinical developments are ongoing for DDLPS [47,48,49] are expected to be effective to both components. On the other hand, clinical genomic testing searching for therapeutic targets are usually conducted using a single tumor sample. In such situation, it is possible that driver alterations specific to either component are selected as potential therapeutic targets. For DDLPS, it is desirable to test two samples derived from both components and target common alterations between both components. Otherwise, therapeutic strategies to simultaneously attack two distinct alterations found in WD and DD components may be necessary.

A limitation of this study is the small number of analyzed cases. It is difficult to estimate actual proportion of early separation-type DDLPS development. In addition, a very few point mutations were detected from WES data, making it difficult to analyze detailed evolutional process. Analyses of more patients using whole genome sequencing will be necessary in the future.

In summary, we report the first multiregion analysis of DDLPS. Our analyses demonstrate very early separation of WD and DD tumor clones and following relatively long clonal selection, at least in some cases of DDLPS. We also found that phylogenetic trees predicted from the genomic alterations were consistent with those predicted from DNA methylation patterns. The expression patterns and DNA methylation patterns of adipogenesis-related genes correlated with each other in each patient. Our results suggest that WD and DD components in DDLPS is formed through characteristic clonal selection with acquisition of different driver genomic alterations and DNA methylation changes.

Materials & Correspondence

Correspondence and requests for materials should be addressed to Naofumi Asano or Hitoshi Ichikawa.

CRediT authorship contribution statement

Tetsuya Sekita: Writing – original draft, Visualization, Formal analysis. **Naofumi Asano:** Supervision, Project administration, Investigation, Funding acquisition, Conceptualization. **Takashi Kubo:** Formal analysis, Data curation. **Hirohiko Totsuka:** Visualization, Formal analysis. **Sachiyo Mitani:** Formal analysis. **Naoko Hattori:** Formal analysis. **Akihiko Yoshida:** Visualization, Investigation. **Eisuke Kobayashi:** Investigation. **Motokiyo Komiyama:** Investigation. **Toshikazu Ushijima:** Formal analysis. **Robert Nakayama:** Supervision. **Masaya Nakamura:** Supervision. **Akira Kawai:** Supervision. **Hitoshi Ichikawa:** Writing – review & editing, Project administration, Funding acquisition, Conceptualization.

Declaration of competing interest

The authors declare no competing interests

Acknowledgements

This study was supported by KAKENHI (21H03062 and 21K15601) of Japan Society of Promotion of Science; by the Grant-in-Aid for Early-Career Scientists from Japan Agency for Medical Research and Development (AMED) (22ck0106537h0003), and by National Cancer Center Research and Development Funds (2020-J-2).

Supplementary materials

Supplementary material associated with this article can be found, in the online version, at doi:10.1016/j.neo.2024.101074.

References

[1] J.R. Goldblum, A.L. Folpe, S.W. Weiss, F.M. Enzinger, Enzinger & Weiss's soft tissue tumors, 7th Edition, Elsevier, 2020.
[2] W.H.O.c.t.e board, Soft tissue and bone tumours, 5th Edition, World Health Organization International Agency for Research on Cancer, 2020.
[3] T. Tamaki, Y. Dong, Y. Ohno, T. Sobue, H. Nishimoto, A. Shibata, The burden of rare cancer in Japan: application of the RARECARE definition, Cancer Epidemiol. 38 (2014) 490–495, https://doi.org/10.1016/j.canep.2014.07.014.
[4] H.L. Evans, Liposarcoma: a study of 55 cases with a reassessment of its classification, Am. J. Surg. Pathol. 3 (1979) 507–523, https://doi.org/10.1097/00000478-197912000-00004.
[5] C.A. Dehner, I.S. Hagemann, J.S.A. Chrisinger, Retroperitoneal dedifferentiated liposarcoma, Am. J. Clin. Pathol. 156 (2021) 920–925, https://doi.org/10.1093/ajcp/aqab051.
[6] A.T.J. Lee, K. Thway, P.H. Huang, R.L. Jones, Clinical and molecular spectrum of liposarcoma, J. Clin. Oncol. 36 (2018) 151–159, https://doi.org/10.1200/JCO.2017.74.9598.
[7] K.M. Dalal, C.R. Antonescu, S. Singer, Diagnosis and management of lipomatous tumors, J. Surg. Oncol. 97 (2008) 298–313, https://doi.org/10.1002/jso.20975.
[8] S.W. Weiss, V.K. Rao, Well-differentiated liposarcoma (atypical lipoma) of deep soft tissue of the extremities, retroperitoneum, and miscellaneous sites. A follow-up study of 92 cases with analysis of the incidence of "dedifferentiation, Am. J. Surg. Pathol. 16 (1992) 1051–1058, https://doi.org/10.1097/00000478-199211000-00003.
[9] A. Amin-Mansour, S. George, S. Sioletic, S.L. Carter, M. Rosenberg, A. Taylor-Weiner, C. Stewart, A. Chevalier, S. Seepo, A. Tracy, et al., Genomic Evolutionary Patterns of Leiomyosarcoma and Liposarcoma, Clin. Cancer Res. 25 (2019) 5135–5142, https://doi.org/10.1158/1078-0432.CCR-19-0271.
[10] H.C. Beird, C.C. Wu, D.R. Ingram, W.L. Wang, A. Alimohamed, C. Gumbs, L. Little, X. Song, B.W. Feig, C.L. Roland, et al., Genomic profiling of dedifferentiated liposarcoma compared to matched well-differentiated liposarcoma reveals higher genomic complexity and a common origin, Cold. Spring. Harb. Mol. Case Stud. 4 (2018), https://doi.org/10.1101/mcs.a002386.
[11] S Sydow, P Piccinelli, S Mitra, P Tsagkozis, A Hesla, C B R De Mattos, J Köster, L Magnusson, J Nilsson, A Ameur, R Wardenaar, F. Foijer, et al., MDM2 amplification in rod-shaped chromosomes provides clues to early stages of circularized gene amplification in liposarcoma, Commun. Biol. 7 (2024) 606, https://doi.org/10.1038/s42003-024-06307-1.
[12] A.M. Crago, N.D. Socci, P. DeCarolis, R. O'Connor, B.S. Taylor, L.X. Qin, C. R. Antonescu, S. Singer, Copy number losses define subgroups of dedifferentiated liposarcoma with poor prognosis and genomic instability, Clin. Cancer Res. 18 (2012) 1334–1340, https://doi.org/10.1158/1078-0432.CCR-11-2820.
[13] A. Italiano, L. Bianchini, F. Keslair, S. Bonnafous, N. Cardot-Leccia, J.M. Coindre, J. M. Dumollard, P. Hofman, A. Leroux, C. Mainguene, et al., HMGA2 is the partner of MDM2 in well-differentiated and dedifferentiated liposarcomas whereas CDK4 belongs to a distinct inconsistent amplicon, Int. J. Cancer 122 (2008) 2233–2241, https://doi.org/10.1002/ijc.23380.
[14] E. Saada-Bouzid, F. Burel-Vandenbos, D. Ranchere-Vince, I. Birtwisle-Peyrottes, B. Chetaille, C. Bouvier, M.C. Chateau, M. Peoc'h, M. Battistella, A. Bazin, et al., Prognostic value of HMGA2, CDK4, and JUN amplification in well-differentiated and dedifferentiated liposarcomas, Mod. Pathol. 28 (2015) 1404–1414, https://doi.org/10.1038/modpathol.2015.96.
[15] Cancer Genome Atlas Research Network, Electronic address, e.d.s.c., and Cancer Genome Atlas Research, N, Comprehensive and integrated genomic characterization of adult soft tissue sarcomas, Cell 171 (2017) 950–965, https://doi.org/10.1016/j.cell.2017.10.014, e928.
[16] M. Hirata, N. Asano, K. Katayama, A. Yoshida, Y. Tsuda, M. Sekimizu, S. Mitani, E. Kobayashi, M. Komiyama, H. Fujimoto, et al., Integrated exome and RNA sequencing of dedifferentiated liposarcoma, Nat. Commun. 10 (2019) 5683, https://doi.org/10.1038/s41467-019-13286-z.

[17] R.A. Burrell, N. McGranahan, J. Bartek, C. Swanton, The causes and consequences of genetic heterogeneity in cancer evolution, Nature 501 (2013) 338–345, https://doi.org/10.1038/nature12625.
[18] H. Zhou, Y. Hu, R. Luo, Y. Zhao, H. Pan, L. Ji, T. Zhou, L. Zhang, H. Long, J. Fu, et al., Multi-region exome sequencing reveals the intratumoral heterogeneity of surgically resected small cell lung cancer, Nat. Commun. 12 (2021) 5431, https://doi.org/10.1038/s41467-021-25787-x.
[19] X. Hua, W. Zhao, A.C. Pesatori, D. Consonni, N.E. Caporaso, T. Zhang, B. Zhu, M. Wang, K. Jones, B. Hicks, et al., Genetic and epigenetic intratumor heterogeneity impacts prognosis of lung adenocarcinoma, Nat. Commun. 11 (2020) 2459, https://doi.org/10.1038/s41467-020-16295-5.
[20] M. Jamal-Hanjani, G.A. Wilson, N. McGranahan, N.J. Birkbak, T.B.K. Watkins, S. Veeriah, S. Shafi, D.H. Johnson, R. Mitter, R. Rosenthal, et al., Tracking the evolution of non-small-cell lung cancer, N. Engl. J. Med. 376 (2017) 2109–2121, https://doi.org/10.1056/NEJMoa1616288.
[21] T.A. Yap, M. Gerlinger, P.A. Futreal, L. Pusztai, C. Swanton, Intratumor heterogeneity: seeing the wood for the trees, Sci. Transl. Med. 4 (2012) 127ps110, https://doi.org/10.1126/scitranslmed.3003854.
[22] M. Gerlinger, A.J. Rowan, S. Horswell, M. Math, J. Larkin, D. Endesfelder, E. Gronroos, P. Martinez, N. Matthews, A. Stewart, et al., Intratumor heterogeneity and branched evolution revealed by multiregion sequencing, N. Engl. J. Med. 366 (2012) 883–892, https://doi.org/10.1056/NEJMoa1113205.
[23] H. Li, R. Durbin, Fast and accurate short read alignment with Burrows-Wheeler transform, Bioinformatics 25 (2009) 1754–1760, https://doi.org/10.1093/bioinformatics/btp324.
[24] K. Cibulskis, M.S. Lawrence, S.L. Carter, A. Sivachenko, D. Jaffe, C. Sougnez, S. Gabriel, M. Meyerson, E.S. Lander, G. Getz, Sensitive detection of somatic point mutations in impure and heterogeneous cancer samples, Nat. Biotechnol. 31 (2013) 213–219, https://doi.org/10.1038/nbt.2514.
[25] J.T. Robinson, H. Thorvaldsdottir, W. Winckler, M. Guttman, E.S. Lander, G. Getz, J.P. Mesirov, Integrative genomics viewer, Nat. Biotechnol. 29 (2011) 24–26, https://doi.org/10.1038/nbt.1754.
[26] P. Van Loo, S.H. Nordgard, O.C. Lingjaerde, H.G. Russnes, I.H. Rye, W. Sun, V. J. Weigman, P. Marynen, A. Zetterberg, B. Naume, et al., Allele-specific copy number analysis of tumors, Proc. Natl. Acad. Sci. USA 107 (2010) 16910–16915, https://doi.org/10.1073/pnas.1009843107.
[27] Y. Shigematsu, T. Niwa, S. Yamashita, H. Taniguchi, R. Kushima, H. Katai, S. Ito, T. Tsukamoto, M. Ichinose, T. Ushijima, Identification of a DNA methylation marker that detects the presence of lymph node metastases of gastric cancers, Oncol. Lett. 4 (2012) 268–274, https://doi.org/10.3892/ol.2012.708.
[28] H. Ishihara, S. Yamashita, Y.Y. Liu, N. Hattori, O. El-Omar, T. Ikeda, H. Fukuda, K. Yoshida, T. Takagi, S. Taneda, et al., Genetic and epigenetic profiling indicates the proximal tubule origin of renal cancers in end-stage renal disease, Cancer Sci. 111 (2020) 4276–4287, https://doi.org/10.1111/cas.14633.
[29] R. Desper, O. Gascuel, Fast and accurate phylogeny reconstruction algorithms based on the minimum-evolution principle, J. Comput. Biol. 9 (2002) 687–705, https://doi.org/10.1089/106652702761034136.
[30] A. Dobin, C.A. Davis, F. Schlesinger, J. Drenkow, C. Zaleski, S. Jha, P. Batut, M. Chaisson, T.R. Gingeras, STAR: ultrafast universal RNA-seq aligner, Bioinformatics 29 (2013) 15–21. 10.1093/bioinformatics/bts635.
[31] A. Subramanian, H. Kuehn, J. Gould, P. Tamayo, J.P. Mesirov, GSEA-P: a desktop application for gene set enrichment analysis, Bioinformatics 23 (2007) 3251–3253, https://doi.org/10.1093/bioinformatics/btm369.
[32] N Gruel, C Quignot, L Lesage, S El Zein, S Bonvalot, D Tzanis, K Ait Rais, F Quinquis, B Manciot, J. Vibert, et al., Cellular origin and clonal evolution of human dedifferentiated liposarcoma, Nat. Commun. 15 (2024) 7941, https://doi.org/10.1038/s41467-024-52067-1.34.
[33] A. Davis, R. Gao, N. Navin, Tumor evolution: Linear, branching, neutral or punctuated? Biochim. Biophys. Acta Rev. Cancer 1867 (2017) 151–161, https://doi.org/10.1016/j.bbcan.2017.01.003.
[34] S.P. Shah, A. Roth, R. Goya, A. Oloumi, G. Ha, Y. Zhao, G. Turashvili, J. Ding, K. Tse, G. Haffari, et al., The clonal and mutational evolution spectrum of primary triple-negative breast cancers, Nature 486 (2012) 395–399, https://doi.org/10.1038/nature10933.
[35] K. Harbst, M. Lauss, H. Cirenajwis, K. Isaksson, F. Rosengren, T. Torngren, A. Kvist, M.C. Johansson, J. Vallon-Christersson, B. Baldetorp, et al., Multiregion whole-exome sequencing uncovers the genetic evolution and mutational heterogeneity of early-stage metastatic melanoma, Cancer Res. 76 (2016) 4765–4774, https://doi.org/10.1158/0008-5472.CAN-15-3476.
[36] M. Vinci, A. Burford, V. Molinari, K. Kessler, S. Popov, M. Clarke, K.R. Taylor, H. N. Pemberton, C.J. Lord, A. Gutteridge, et al., Functional diversity and cooperativity between subclonal populations of pediatric glioblastoma and diffuse intrinsic pontine glioma cells, Nat. Med. 24 (2018) 1204–1215, https://doi.org/10.1038/s41591-018-0086-7.
[37] E.L. Snyder, D.J. Sandstrom, K. Law, C. Fiore, E. Sicinska, J. Brito, D. Bailey, J. A. Fletcher, M. Loda, S.J. Rodig, et al., c-Jun amplification and overexpression are oncogenic in liposarcoma but not always sufficient to inhibit the adipocytic differentiation programme, J. Pathol. 218 (2009) 292–300, https://doi.org/10.1002/path.2564.
[38] O. Mariani, C. Brennetot, J.M. Coindre, N. Gruel, C. Ganem, O. Delattre, M. H. Stern, A Aurias, JUN oncogene amplification and overexpression block adipocytic differentiation in highly aggressive sarcomas, Cancer Cell 11 (2007) 361–374, https://doi.org/10.1016/j.ccr.2007.02.007.
[39] T.W. Fawcett, H.B. Eastman, J.L. Martindale, N.J. Holbrook, Physical and functional association between GADD153 and CCAAT/enhancer-binding protein β during cellular stress, J. Biol. Chem. 271 (1996) 14285–14289.
[40] C.V. Angeles, A. Velez, J. Rios, B. Laxa, D. Shum, P.D. Ruiz, Y. Shen, I. Ostrovnaya, R. Gularte-Merida, B.A. Nacev, et al., A high-content screen for c/ebpalpha expression identifies novel therapeutic agents in dedifferentiated liposarcoma, Clin. Cancer Res. 28 (2022) 175–186, https://doi.org/10.1158/1078-0432.CCR-19-2486.
[41] D. Brocks, Y. Assenov, S. Minner, O. Bogatyrova, R. Simon, C. Koop, C. Oakes, M. Zucknick, D.B. Lipka, J. Weischenfeldt, et al., Intratumor DNA methylation heterogeneity reflects clonal evolution in aggressive prostate cancer, Cell Rep. 8 (2014) 798–806, https://doi.org/10.1016/j.celrep.2014.06.053.
[42] D. Richard, F. Picard, Brown fat biology and thermogenesis, Front. Biosci. (Landmark. Ed) 16 (2011) 1233–1260, https://doi.org/10.2741/3786.
[43] L. Han, B. Wang, R. Wang, S. Gong, G. Chen, W. Xu, The shift in the balance between osteoblastogenesis and adipogenesis of mesenchymal stem cells mediated by glucocorticoid receptor, Stem Cell Res. Ther. 10 (2019) 377, https://doi.org/10.1186/s13287-019-1498-0.
[44] K. Nakajima, T. Kidani, H. Miura, Molecular profiling of bone remodeling occurring in musculoskeletal tumors, J. Orthop. Res. 39 (2021) 1402–1410, https://doi.org/10.1002/jor.24879.
[45] M. Okamura, H. Kudo, K. Wakabayashi, T. Tanaka, A. Nonaka, A. Uchida, S. Tsutsumi, I. Sakakibara, M. Naito, T.F. Osborne, et al., COUP-TFII acts downstream of Wnt/beta-catenin signal to silence PPARgamma gene expression and repress adipogenesis, Proc. Natl. Acad. Sci. USA 106 (2009) 5819–5824, https://doi.org/10.1073/pnas.0901676106.
[46] S. Shaik, E.C. Martin, D.J. Hayes, J.M. Gimble, R.V. Devireddy, Transcriptomic profiling of adipose derived stem cells undergoing osteogenesis by RNA-Seq, Sci. Rep. 9 (2019) 11800, https://doi.org/10.1038/s41598-019-48089-1.
[47] P. LoRusso, N. Yamamoto, M.R. Patel, S.A. Laurie, T.M. Bauer, J. Geng, T. Davenport, M. Teufel, J. Li, M. Lahmar, M.M. Gounder, The MDM2-p53 antagonist brigimadlin (BI 907828) in patients with advanced or metastatic solid tumors: results of a phase Ia, first-in-human, dose-escalation study, Cancer Discov. 13 (2023) 1802–1813, https://doi.org/10.1158/2159-8290.CD-23-0153.
[48] T. Assi, J. Kattan, E. Rassy, H. Nassereddine, F. Farhat, C. Honore, A. Le Cesne, J. Adam, O. Mir, Targeting CDK4 (cyclin-dependent kinase) amplification in liposarcoma: a comprehensive review, Crit. Rev. Oncol. Hematol. 153 (2020) 103029, https://doi.org/10.1016/j.critrevonc.2020.103029.
[49] N Somaiah, W. Tap, MDM2-p53 in liposarcoma: The need for targeted therapies with novel mechanisms of action, Cancer Treat. Rev. 122 (2024) 102668, https://doi.org/10.1016/j.critrevonc.2023.102668.